2

Design multifunctional product by nanostructures

Agić Ante and Mijović Budimir
Faculty of Chemical Engineering and Technology, Zagreb, Croatia
Faculty of Textile Technology, Zagreb, Croatia

1. Introduction

The largest variety of efficient and elegant multifunctional materials is seen in natural biological systems, which occur sometimes in the simple geometrical forms in man-made materials. The multifunctionality of a material could be achieved by designing the material from the micro to macroscales (bottom up design approach), mimicking the structural formations created by nature [1]. Biological materials present around us have a large number of ingenious solutions and serve as a source of inspiration. There are different ways of producing multifunctional materials that depend largely on whether these materials are structural composites, smart materials, or nanostructured materials. The nanostructure materials are most challenging and innovative processes, introducing, in the manufacturing, a new approaches such as self-assembly and self-replication. For bio-materials involved in surface-interface related processes, common geometries involve capillaries, dendrites, hair, or fin-like attachments supported on larger substrates. It may be useful to incorporate similar hierarchical structures in the design and fabrication of multifunctional synthetic products that include surface sensitive functions such as sensing, reactivity, charge storage, transport property or stress transfer. Significant effort is being directed in order to fabricate and understand materials involving multiple length scales and functionalities. Porous fibrous structures can behave like lightweight solids providing significantly higher surface area compared to compact ones. Depending on what is attached on their surfaces, or what matrix is infiltrated in them, these core structures can be envisioned in a wide variety of surface active components or net-shape composites. If nanoelements can be attached in the pores, the surface area within the given space can be increased by several orders of magnitude, thereby increasing the potency of any desired surface functionality. Recent developments in electrospinning have made these possible, thanks to a coelectrospinning polymer suspension [2]. This opens up the possibility of taking a functional material of any shape and size, and attaching nanoelements on them for added surface functionality. The fast growing nanotechnology with modern computational/experimental methods give the possibility to design multifunctional materials and products in human surroundings. Smart clothing, portable fuel cells, medical devices are some of them. Research in nanotechnology began with applications outside of everyday life and is based on discoveries in physics and chemistry. The reason for that is need to understand the physical and chemical properties of

molecules and nanostructures in order to control them. For example, nanoscale manipulation results in new functionalities for textile structures, including self-cleaning, sensing, actuating, and communicating. Development of precisely controlled or programmable medical nanomachines and nanorobots is great promise for nanomedicine. Once nanomachines are available, the ultimate dream of every medical man becomes reality. The miniaturisation of instruments on micro- and nano-dimensions promises to make our future lives safer with more humanity. A new approach in material synthesis is a computational-based material development. It is based on multiscale material and process modelling spanning, on a large spectrum of time as well as on length scales. Multi-scale materials design means to design materials from a molecular scale up to a macro scale. The ability to manipulate at atomic and molecular level is also creating materials and structures that have unique functionalities and characteristics. Therefore it will be and revolutionizing next-generation technology ranging from structural materials to nano-electro-mechanical systems (NEMs), for medicine and bioengineering applications. Recent research development in nanomaterials has been progressing at a tremendous speed for it can totally change the ways in which materials can be made with unusual properties. Such research includes the synthetic of nanomaterials, manufacturing processes, in terms of the controls of their nano-structural and geometrical properties, mouldability and mixability with other matrix for nanocomposites. The cost of designing and producing a novel multifunctional material can be high and the risk of investment to be significant. Computational materials research that relies on multi-scale modelling has the potential to significantly reduce development costs of new nanostructured materials for demanding applications by bringing physical and microstructural information into the realm of the design engineer. As there are various potential applications of nanotechnology in design multifunctional product, only some of the well-known properties come from by nano-treatment are critically highlighted. This chapter review current research in nanotechnology application of the electrospinning nanofiber, from fibber production and development to end uses as multifunctional nanostructure device and product. The electrospinning phenomena are described from experimental point of view to it simulation as multiscale problem.

2. The multifunctional materials and products

2.1 Responsive nanoparticles

There are several directions in the research and development of the responsive nanoparticle (RNP) applications . Development of particles that respond by changing stability of colloidal dispersions is the first directions. Stimuli-responsive emulsions and foams could be very attractive for various technologies in coating industries , cosmetic, and personal care. The RNPs compete with surfactants and, hence, the costs for the particle production will play a key role. The main challenge is the development of robust and simple methods for the synthesis of RNPs from inexpensive colloidal particles and suspensions. That is indeed not a simple job since most of commercially available NPs are more expensive than surfactants. Another important application of RNPs for tunable colloidal stability of the particle suspensions is a very broad area of biosensors.

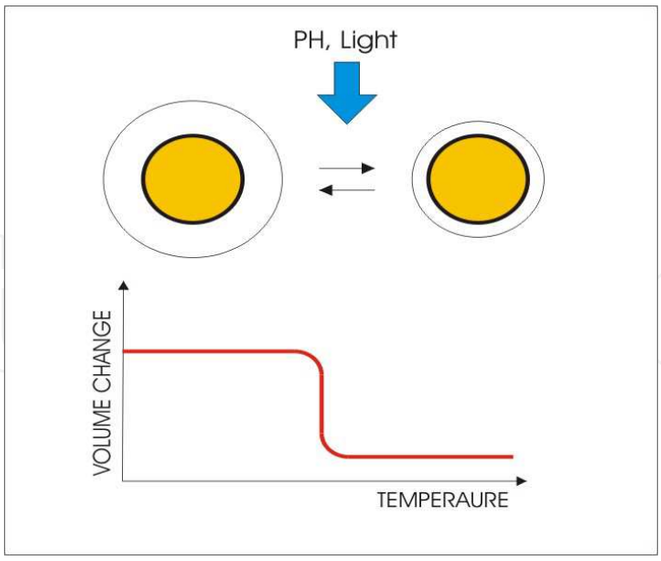

Fig. 1. Stimuli-responsive nanoparticles

The second direction is stimuli-responsive capsules that can release the cargo upon external stimuli (See Fig. 1). The capsules are interesting for biomedical applications (drugs delivery agents) and for composite materials (release of chemicals for self-healing). The most challenging task in many cases is to engineering systems capable to work with demanded stimuli. It is not a simple job for many biomedical applications where signalling biomolecules are present in very small concentrations and a range of changes of many properties is limited by physiological conditions. A well-known challenge is related to the acceptable size production of capsules. Many medical applications need capsules less than 50 nm in diameter. Fabrication of capsules with a narrow pore size distribution and tunable sizes could dramatically improve the mass transport control. A hierarchically organized multicompartment RNPs are in the focus. These particles could respond to weak signals, to multiple signals, and could demonstrate a multiple response. They can perform logical operations with multiple signals, store energy, absorb and consume chemicals, and synthesize and release chemicals. In other words, they could operate as an autonomous intelligent minidevice. The development of such RNPs can be considered as a part of biomimetics inspired by living cells or logic extension of the bottom up approach in nanotechnology. The development of the intelligent RNPs faces numerous challenges related to the coupling of many functional building blocks in a single hierarchically structured RNP. These particles could find applications for intelligent drug delivery, removal of toxic substances, diagnostics in medicine, intelligent catalysis, microreactors for chemical synthesis and biotechnology, new generation of smart products for personal use, and others.

2.2 Nanocoatings

In general, the coating's thickness is at least an order of magnitude lower than the size of the geometry to be coated. The coating's thickness less than 10 nm is called nanocoating. Nano-coatings are materials that are produced by shrinking the material at the molecular level to form a denser product. Nanostmcture coatings have an excellent toughness, good corrosion resistance, wear and adhesion properties. These coatings can be used to repair component

parts instead of replacing them, resulting in significant reductions in maintenance costs. Additionally, the nanostructure coatings will extend the service life of the component due to the improved properties over conventional coatings.

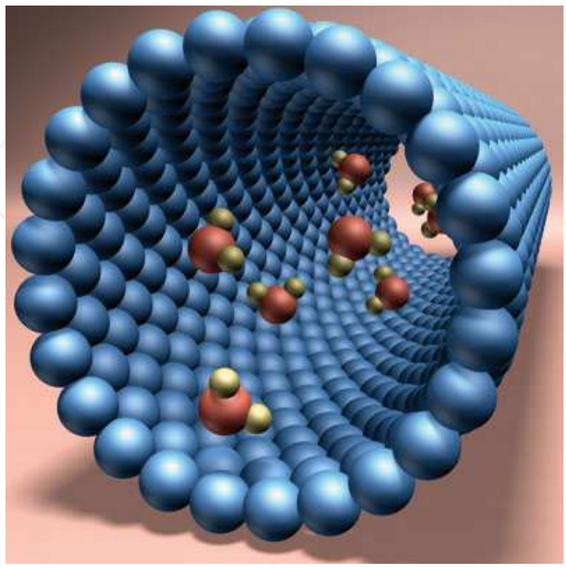

Fig. 2. Nanocoatings

2.3 Fibrous nanostructure

The nanofibers are basic building block for plants and animals. From the structural point of view, a uniaxial structure is able to transmit forces along its length and reducing required mass of materials. Nanofibers serves as the another platform for multifunctional hierarchical example. The successful design concepts of nature, the nanofiber becomes an attractive basic building component in the construction of hierarchically organized nanostructures. To follow nature's design, a process that is able to fabricate nanofiber from a variety materials and mixtures is a prerequisite. Control of the nanofibers arrangement is also necessary to optimize structural requirements. Finally, incorporation of other components into the nanofibers is required to form a complex, hierarchically organized composite. A nanofiber fabrication technique known as electrospinning process has the potential to play a vital role in the construction of a multi-levels nanostructure [3].

In this paper, we will introduce electrospinning as a potential technology for use as a platform for multifunctional, hierarchically organized nanostructures. Electrospinning is a method of producing superfine fibers with diameters ranging from 10 nm to 100 nm. Electrospinning occurs when the electrical forces at the surface of a polymer solution overcome the surface tension and cause an electrically charged jet of polymer solution to be ejected. A schematic drawing of the electrospinning process is shown in Figure 3. The electrically charged jet undergoes a series of electrically induced instabilities during its passage to the collection surface which results in complicated stretching and looping of the jet [4]. This stretching process is accompanied by the rapid evaporation of the solvent molecules, further reducing the jet diameter. Dry fibers are accumulated on the surface of the collector, resulting in a non-woven mesh of nanofibers.

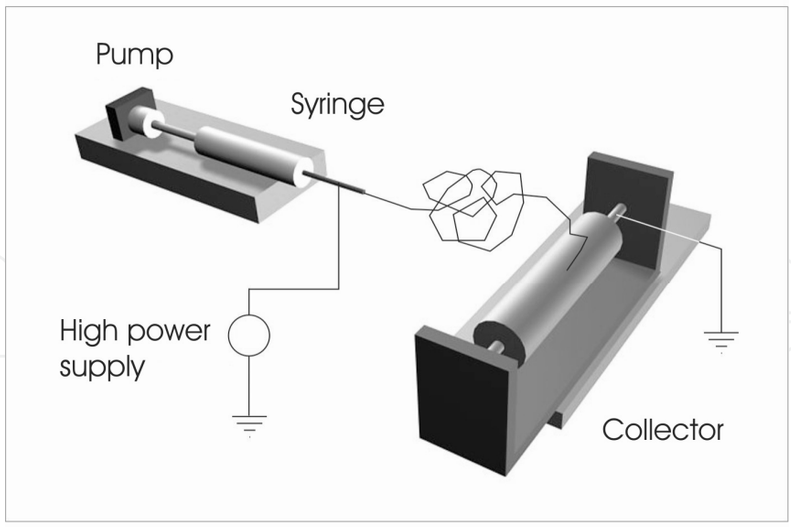

Fig. 3. The electrospinning process

Basically, an electrospinning system consists of three major components: a high voltage power supply, an emitter (e.g., a syringe) and a grounded collecting plate (usually a metal screen, plate, or rotating mandrel). There are a wide range of polymers that used in electrospinning and are able to form fine nanofibers within the submicron range and used for varied applications. Electrospun nanofibers have been reported as being from various synthetic polymers, natural polymers or a blend of both including proteins, nucleic acids [5] .
The electrospinning process is solely governed by many parameters, classified broadly into rheological, processing, and ambient parameters. Rheological parameters include viscosity, conductivity, molecular weight, and surface tension and process parameters include applied electric field, tip to collector distance and flow rate. Each of these parameters significantly affect the fibers morphology obtained as a result of electrospinning, and by proper manipulation of these parameters we can get nanofibers fabrics of desired structure and properties on multiple material scale . Among these variables, ambient parameters encompass the humidity and temperature of the surroundings which play a significant role in determining the morphology and topology of electrospun fabrics. Nanofibrous assemblies such as non-woven fibrous sheet, aligned fibrous fabric, continuous yarn and 3D structure have been fabricated using electrospinning . Physical characteristics of the electrospun nanofibers can also be manipulated by selecting the electrospinning conditions and solution. Structure organization on a few hierarchical levels (See Fig. 4) has been developed using electrospinning. Such hierarchy and multifunctionality potential will be described in the following sections. Finally, we will describe how electrospun multifunctional, hierarchically organized nanostructure can be used in applications such as healthcare, defence and security, and environmental.

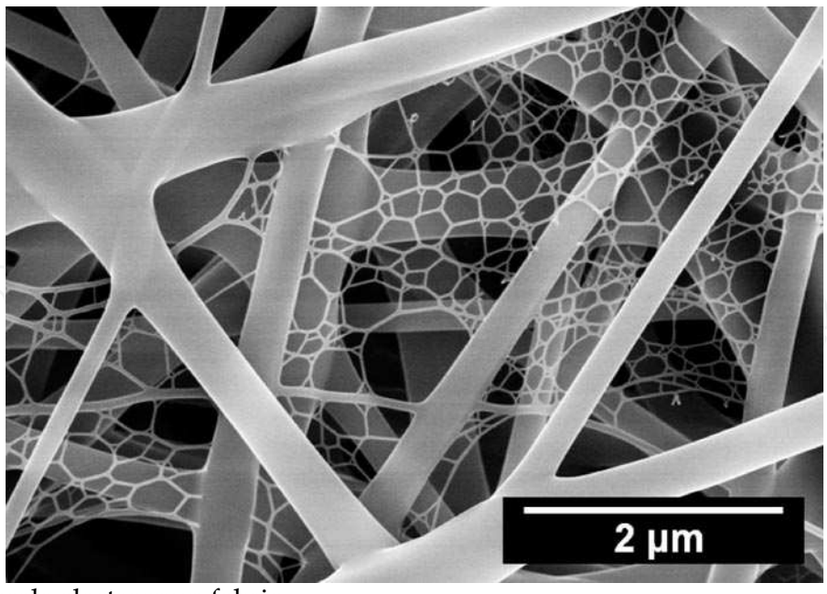

Fig. 4. Multiscale electrospun fabric

3. Fundamentals of electrospinning

The slender-body approximation is widely used in electrospinning analysis of common fluids [4]. The presence of nanoelements (nanoparticles, carbon nanotube, clay) in suspension jet complicate replacement 3D axisymetric with 1D equivalent jet problem under solid-fluid interaction force on nanolevel domain. The applied electric field induced dipole moment, while torque on the dipole rotate and align the nanoelement with electric field. The theories developed to describe the behaviour of the suspension jet fall into two levels macroscopic and microscopic. The macroscopic governing equations of the electrospinning are equation of continuity, conservation of the charge, balance of momentum and electric field equation. Conservation of mass for the jet requires that [4]

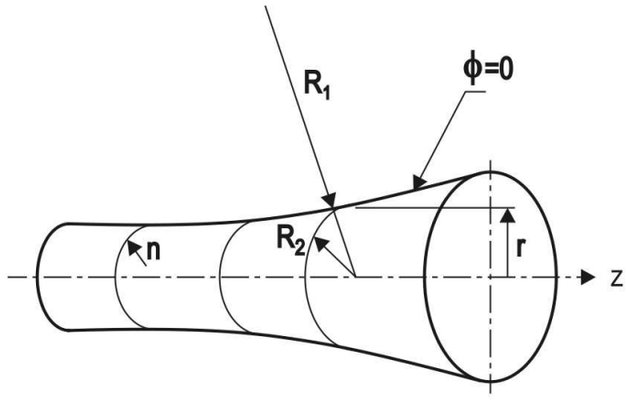

Fig. 5. Geometry of the Jet flow

$$\frac{\partial}{\partial t}\left(\pi r^2\right)+\frac{\partial}{\partial z}\left(\pi r^2 v\right)=0 \tag{1}$$

where r is jet radius, and v is effective velocity. The conservation of charge may be expressed as

$$\frac{\partial}{\partial t}\left(2\pi r\sigma\right)+\frac{\partial}{\partial z}\left(\pi r^2 K E+2\pi r\sigma\right)=0 \tag{2}$$

where E the axial component of the electric field is, K is the effective electrical conductivity of the jet, and σ is the surface charge density. The momentum equation for the fluid can be derived as follow

$$\rho\left(\frac{\partial v}{\partial t}+v\frac{\partial v}{\partial z}\right)=\rho\cdot g+\frac{\partial}{\partial z}\left(\tau_{zz}-\tau_{rr}\right)+\frac{\gamma}{r^2}\frac{\partial r}{\partial z}+\frac{\sigma}{\varepsilon_0}\frac{\partial\sigma}{\partial z}+\left(\varepsilon-\varepsilon_0\right)\cdot E\frac{\partial E}{\partial z}+\frac{2\sigma}{r}E \tag{3}$$

where ρ is fluid density, respectively. The τ_{ij} deviatoric stress tensor in fluid, γ is the surface tension, ε and ε_0 are the effective dielectric constants of the jet and ambient air respectively. Tangential component (effective) of electric field inside the jet has the form [4]

$$E=E_\infty-\left[\frac{1}{\varepsilon}\frac{\partial}{\partial z}\left(\sigma\cdot r\right)-\frac{1}{2}\left(\frac{\varepsilon}{\varepsilon_0}-1\right)\frac{\partial^2}{\partial z^2}\left(Er^2\right)\right]\cdot\ell n\left(\frac{L}{r_0}\right) \tag{4}$$

where r_0 is initial jet radius, L is characteristic scale length, E_∞ is the externally imposed constant electric field. For polymer suspension stress tensor τ_{ij} come from polymeric $\hat{\tau}_{ij}$ and solvent contribution tensor via constitutive equation

$$\tau_{ij}=\hat{\tau}_{ij}+\eta_s\cdot\dot{\gamma}_{ij} \tag{5}$$

where η_s is solvent viscosity, and $\dot{\gamma}_{ij}$ strain rate tensor. The polymer contribution tensor $\hat{\tau}_{ij}$ depend on microscopic models of the suspension. Microscopic approach represents the microstructural features of material by means of a large number of micromechanical elements (beads, platelet, rods) obeying stochastic differential equations. The evolution equations of the microelements arise from a balance of momentum on the elementary level. For example, rheological behavior of the dilute suspension of the carbon nanotube (CNTs) in polymer matrix can be described as FENE dumbbell model [6]

$$\lambda\left\langle Q\cdot Q\right\rangle^{\nabla}=\delta_{ij}-\frac{c\left\langle Q.Q\right\rangle}{1-tr\left\langle Q.Q\right\rangle/b_{\max}} \tag{6}$$

where $\langle Q \cdot Q \rangle$ is the suspension configuration tensor (See Fig. 6), c is a spring constant, and $b_{\max}$ is maximum CNT extensibility. Subscript ∇ represent the upper convected derivative,

$$A^{\nabla} = \frac{d}{dt} A - (\nabla v)^{T} \cdot A - A \cdot (\nabla v)$$

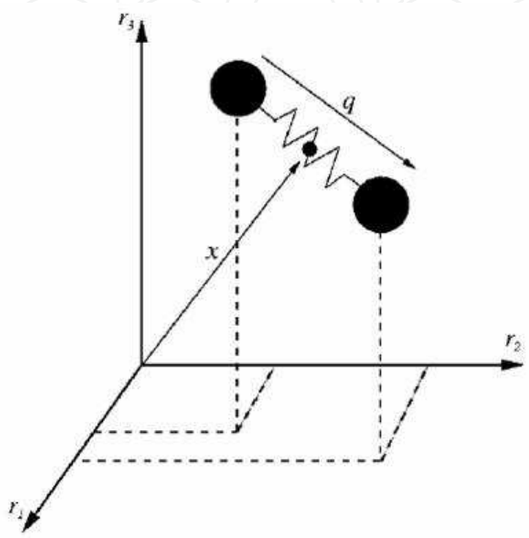

Fig. 6. FENE dumbbell model

and λ denote a relaxation time. The polymeric stress can be obtained from the following relation

$$\frac{\hat{\tau}_{ij}}{nkT} = \delta_{ij} - \frac{c\langle Q.Q \rangle}{1 - tr\langle Q.Q \rangle / b_{\max}} \tag{7}$$

where k is Boltzmann's constant, T is temperature, and n is dumbbells density. Orientation probability distribution function ψ of the dumbbell vector Q can be described by the Fokker-Planck equation, neglecting rotary diffusivity.

$$\frac{\partial \psi}{\partial t} + \frac{\partial}{\partial Q}(\psi \cdot Q) = 0 \tag{8}$$

Solution equations (7) and (8) with supposition that flow in orifice is Hamel flow [7], give value orientation probability distribution function ψ along streamline of the jet. Rotation motion of a nanoelement (CNTs for example) in a Newtonian flow can be described as short fiber suspension model as another rheological model [8]

$$\frac{dp}{dt} = \frac{1}{2}\omega_{ij} p_j + \frac{1}{2}\Theta\left(\frac{d\gamma_{ij}}{dt} p_j - \frac{d\gamma_{kl}}{dt} p_k p_l p_i\right) - D_r \frac{1}{\psi}\frac{\partial \psi}{\partial t} \tag{9}$$

where p is a unit vector in nanoelement axis direction, ω_{ij} is the rotation rate tensor, γ_{ij} is the deformation tensor, D_r is the rotary diffusivity and Θ is shape factor. Microscopic models for evolution of suspension microstructure can be coupled to macroscopic transport equations of mass and momentum to yield micro-macro multiscale flow models. The presence of the CNTs in the solution contributes to new form of instability with influences on the formation of the electrospun mat. The high strain rate on the nanoscale with complicated microstructure requires innovative research approach from the computational modelling point of view [9].

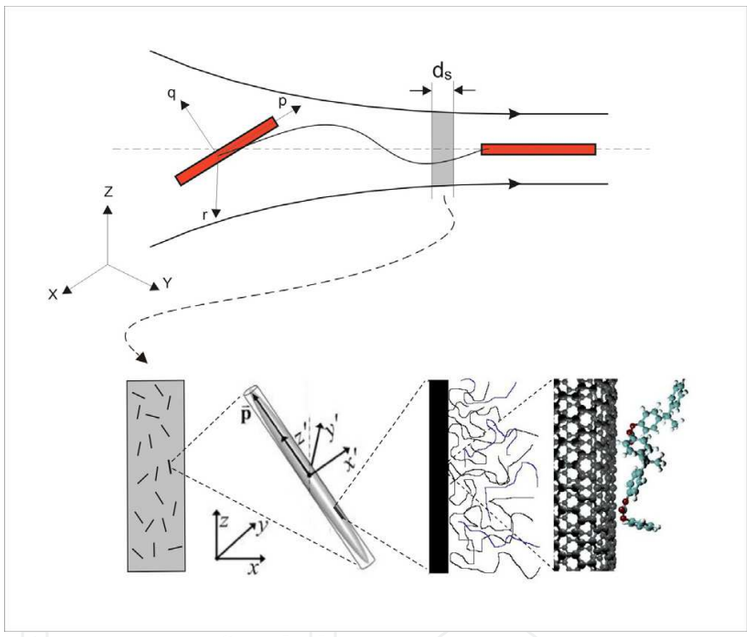

Fig. 7. The CNTs alignment in jet flow [10]

By the Fig. 6 illustrated multiscale treatment the CNTs suspension in the jet , one time as short flexible cylinder in solution (microscale), and second time as coarse grain system with polymer chain particles and CNT(nanoscale level).

4. Multifunctional nanofiber-based structure

The variety of materials and fibrous structures that can be electrospun allow for the incorporation and optimization of various functions to the nanofiber, either during spinning or through post-spinning modifications. A schematic of the multi-level organization of an electrospun fiber based composite is shown in Fig. 8.

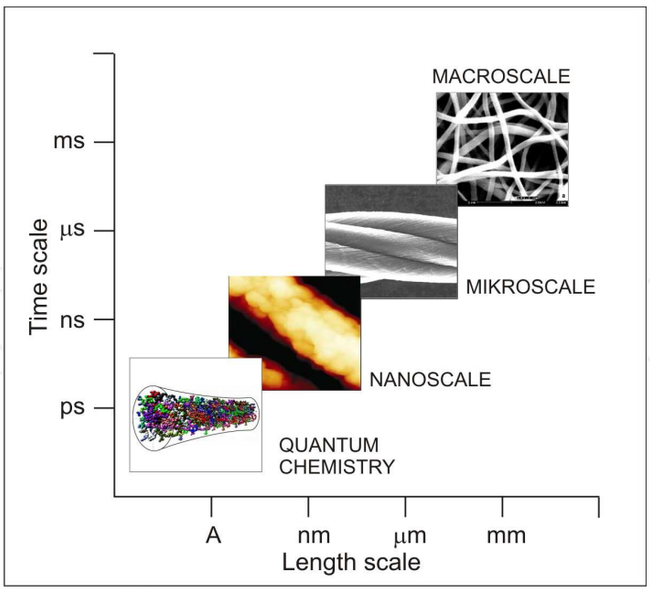

Fig. 8. Multiscale electrospun fabrics

Based on current technology, at least four different levels of organization can be put together to form a nanofiber based hierarchically organized structure. At the first level, nanoparticles or a second polymer can be mixed into the primary polymer solution and electrospun to form composite nanofiber. Using a dual-orifice spinneret design, a second layer of material can be coated over an inner core material during electrospinning to give rise to the second level organization. Two solution reservoirs, one leading to the inner orifice and the other to the outer orifice will extrude the solutions simultaneously. Otherwise, other conditions for electrospinning remain the same. Rapid evaporation of the solvents during the spinning process reduces mixing of the two solutions therefore forming core-shell nanofiber. At the same level, various surface coating or functionalization techniques may be used to introduce additional property to the fabricated nanofiber surface. Chemical functionality is a vital component in advance multi-functional composite material to detect and respond to changes in its environment. Thus various surface modifications techniques have been used to construct the preferred arrangement of chemically active molecules on the surface with the nanofiber as a supporting base. The third level organization will see the fibers oriented and organized to optimize its performance. A multi-layered nanofiber membrane or mixed materials nanofibers membrane can be fabricated *in situ* through selective spinning or using a multiple orifice spinneret design, respectively. Finally, the nanofibrous assembly may be embedded within a matrix to give the fourth-level organization. The resultant structure will have various properties and functionality due its hierarchical organization. Nanofiber structure at various levels have been constructed and tested for various applications and will be covered in the following sections. To follow surface functionality and modification, jet flow must be solved on multiple scale level. All above scale (nanoscale) can be solved by use particle method together with coarse grain method on supramolecular level.

4.1 Nanofiber effective properties

The effective properties of the nanofiber can be determined by homogenization procedure using representative volume element (RVE). There is need for incorporating more physical information on microscale in order to precise determine material behaviour model. For electrospun suspension with nanoelements (CNTs,..), a concentric composite cylinder embedded with a caped carbon nanotube represents RVE as shown by Fig 9. A carbon nanotube with a length 2ℓ, radii $2a$ is embedded at the centre of matrix materials with a radii R and length 2L.

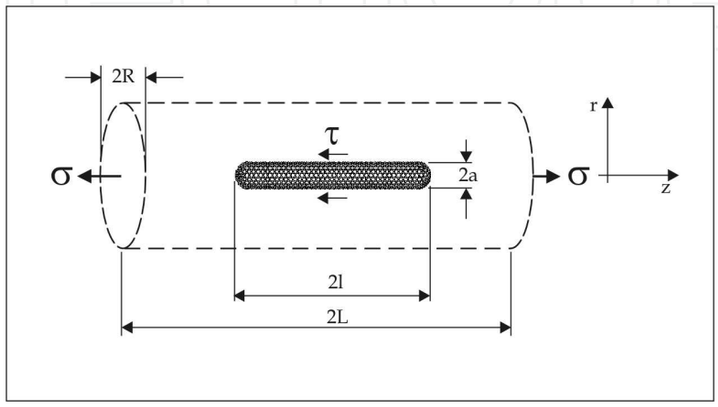

Fig. 9. The nanofiber representative volume element

The discrete atomic nanotube structure replaced the effective (solid) fiber having the same length and outer diameter as a discrete nanotube with effective Young's nanotube modulus determined from atomic structure. The stress and strain distribution in RVE was determined using modified shear-lag model [11]. For the known stress and strain distribution under RVE we can calculate elastic effective properties quantificators. The effective axial module E_{33}, and the transverse module $E_{11} = E_{22}$, can be calculated as follow

$$E_{33} = \frac{\langle \sigma_{zz} \rangle}{\langle \varepsilon_{zz} \rangle}$$
$$E_{11} = \frac{\langle \sigma_{xx} \rangle}{\langle \varepsilon_{xx} \rangle} \tag{10}$$

where $\langle \ \rangle$ denotes a volume average under volume V as defined by

$$\langle \Xi \rangle = \frac{1}{V} \int_V \Xi(x, y, z) \cdot dV \ . \tag{11}$$

The thre-phase concentric cylindrical shell model has been proposed to predict effective modulus of nanotube reinforced nanofibers [12]. The modulus of nanofiber depend strongly upon the thickness of the interphase and CNTs diameter (See Fig. 10).

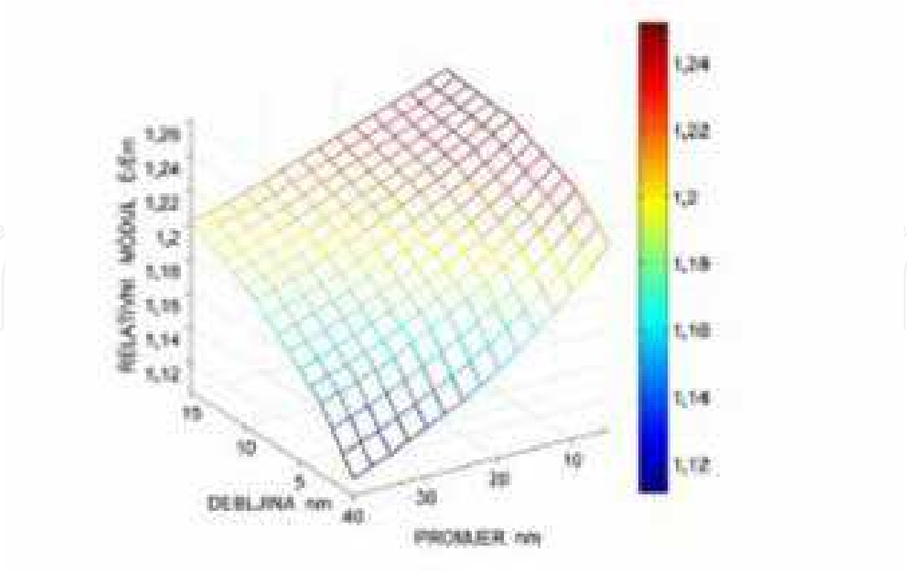

Fig. 10. Modulus dependence on interphase and CNT diameter

4.2 Network macroscopic properties

Macroscopic properties of the multifunctional structure determine final value of the any engineering product. The major objective in the determination of macroscopic properties is the link between atomic and continuum types of modelling and simulation approaches. The multiscale method such as quasi-continuum, bridge method, coarse-grain method, and dissipative particle dynamics are some popular methods of solution [9],[13]. The main advantage of the mesoscopic model is its higher computational efficiency than the molecular modelling without a loss of detailed properties at molecular level. Peridynamic modelling of fibrous network is another promising method, which allows damage, fracture and long-range forces to be treated as natural components of the deformation of materials [14]. In the first stage, effective fiber properties are determined by homogenization procedure, while in the second stage the point-bonded stochastic fibrous network at mesoscale is replaced by continuum plane stress model. Effective mechanical properties of nanofiber sheets at the macro scale level can be determined using the 2D Timoshenko beam-network. The critical parameters are the mean number of crossings per nanofiber, total nanofiber crossing in sheet and mean segment length [15]. Let as first consider a general planar fiber network characterized by fibre concentration n and fibre angular and length distribution $\psi(\phi,\ell)$, where ϕ and ℓ are fibre orientation angle and fibre length, respectively. The fibre radius r is considered uniform and the fibre concentration n is defined as the number of fiber per unit area.

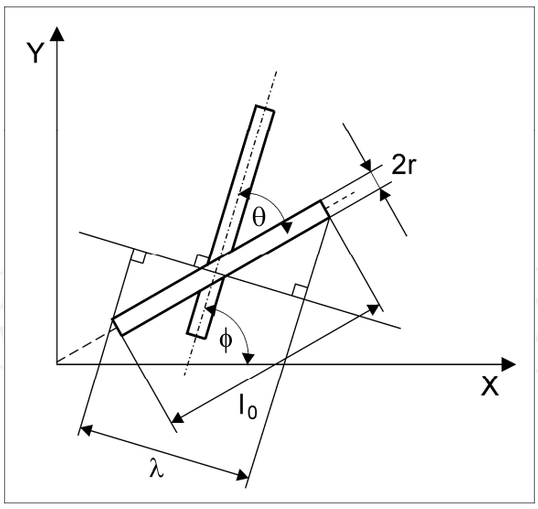

Fig. 11. The fiber contact analysis

The Poisson probability distribution can be used to describe the fiber segment length distribution for electrospun fabrics, a portion of the fiber between two neighbouring contacts:

$$f(\ell) = \frac{1}{\bar{\ell}} \exp\left(-\ell/\bar{\ell}\right) \tag{12}$$

where $\bar{\ell}$ is the mean segment length. The total number fibre segments $\hat{N}$ in the rectangular region $b \times h$

$$\hat{N} = \left\{n \cdot \ell_0 \left(\langle\lambda\rangle + 2r\right) - 1\right\} \cdot n \cdot b \cdot h \tag{13}$$

with $\langle\lambda\rangle = \int_0^{\phi} \int_0^{\infty} \psi(\vartheta, \ell) \cdot \lambda(\vartheta) \cdot d\ell \cdot d\vartheta$

where the dangled segments at fiber ends have been excluded. The fiber network will be deformed in several ways. The strain energy in fiber segments come from bending, stretching and shearing modes of deformation (see Figure 12)

$$\begin{aligned} U &= n \cdot \ell_0 \cdot b \cdot h \frac{1}{2} \iint \frac{E \cdot A}{\ell} \varepsilon_{xx}^2 \cdot \psi(\varphi, \ell) \cdot \ell \cdot d\ell \cdot d\varphi \\ &+ n \cdot \left\{n \cdot \ell_0 \cdot \left(\langle\lambda\rangle + 2r\right) - 1\right\} \cdot b \cdot h \cdot \frac{1}{2} \left\{ \iint \frac{G \cdot A}{\ell} \cdot \cdot \gamma_{xy}^2 \cdot \psi(\varphi, \ell) \cdot \ell \cdot d\ell \cdot d\varphi \right. \\ &\left. + \iint \frac{3 \cdot E \cdot I}{\ell^3} \gamma_{xy}^2 \cdot \psi(\varphi, \ell) \cdot \ell \cdot d\ell \cdot d\varphi \right\} \end{aligned} \tag{14}$$

where A and I are beam cross-section area and moment of inertia, respectively. The first term on right side is stretching mode, while second and last term are shear bending modes respectively.

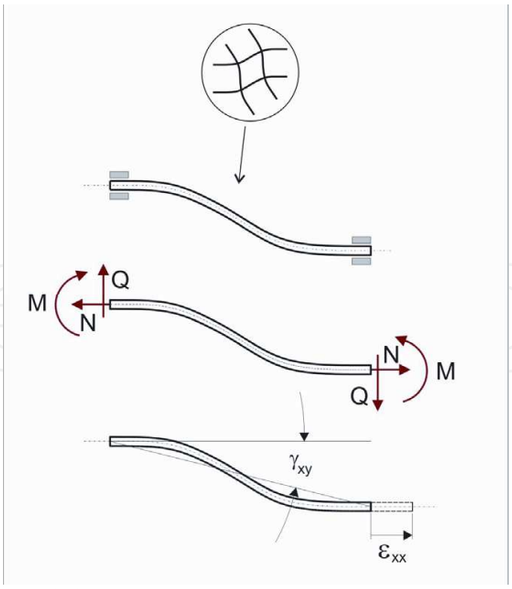

Fig. 12. Fiber network 2D model

The effective material constants for fiber network can be determined using homogenization procedure concept for fiber network. The strain energy fiber network for representative volume element is equal to strain energy continuum element with effective material constant. The strain energy of the representative volume element under plane stress conditions are

$$U = \frac{1}{2} \cdot \left\langle \varepsilon_{ij} \right\rangle \cdot C_{ijkl} \left\langle \varepsilon_{kl} \right\rangle \cdot V \tag{15}$$

where is $V = b \cdot h \cdot 2 \cdot r$ - representative volume element , C_{ijkl} are effective elasticity tensor. The square bracket $\langle \ \rangle$ means macroscopic strain value. We assume that microscopic deformation tensor of a fiber segments ε_{ij} is compatible with effective macroscopic strain $\left\langle \varepsilon_{ij} \right\rangle$ of effective continuum (affine transformation). This is bridge relations between fiber segment microstrain ε_{ij} and macroscopic strain $\left\langle \varepsilon_{ij} \right\rangle$ in the effective medium. Properties of this nanofibrous structure on the macro scale depend on the 3D joint morphology. The joints can be modelled as contact torsional elements with spring and dashpot [15]. The elastic energy of the whole random fibre network can be calculated numerically, from the local deformation state of the each segment by finite element method [16]. The elastic energy of the network is then the sum of the elastic energies of all segments. We consider here tensile stress, and the fibers are rigidly bonded to each other at every fibre-fibre crossing points. To mimic the microstructure of electrospun mats, we generated fibrous structures with fibers positioned in horizontal planes, and stacked the planes on top of one another to form a 2D or 3D structure. The representative volume element dimensions are considered to be an input parameter that can be used among other parameters to control the solid volume fraction of the structure, density number of fibre in the simulations. The

number of intersections/unit area and mean lengths are obtained from image analysis of electrospun sheets. For the random point field the stochastic fiber network was generated. Using polar coordinates and having the centreline equation of each fiber, the relevant parameters confined in the simulation box is obtained. The procedure is repeated until reaching the desired parameters is achieved. The non-load bearing fiber segments were removed and trimmed to keep dimensions $b \times h$ of the representative window (see Fig. 13). A line representative network model is replaced by finite element beam mesh. The finite element analyses were performed in a network of 100 fibers, for some CNTs volume fractions values. Nanofibers were modelled as equivalent cylindrical beam as mentioned above. Effective mechanical properties of nanofiber sheets at the macro scale level can be determined using the 2D Timoshenko beam-network.

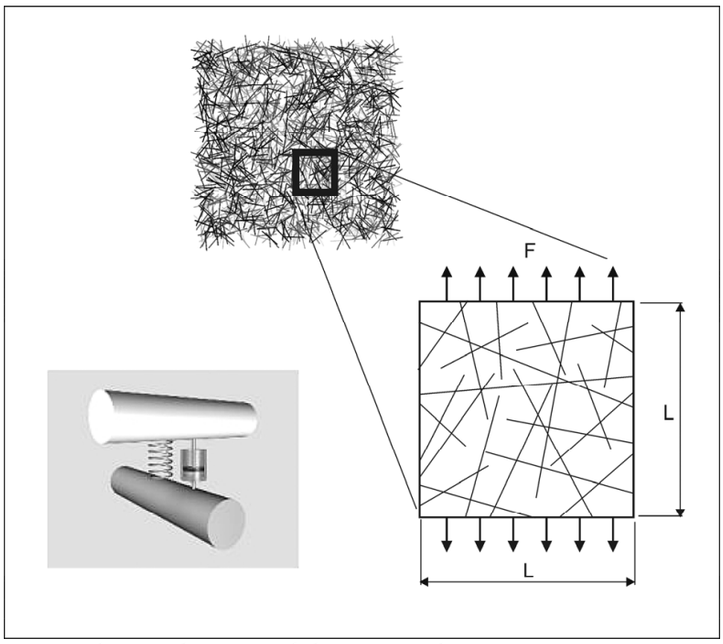

Fig. 13. Repesentative volume element of the network

For a displacement-based form of beam element, the principle of virtual work is assumed valid. For a beam system, a necessary and sufficient condition for equilibrium is that the virtual work done by sum of the external forces and internal forces vanish for any virtual displacement $\delta W = 0$. *The W* is the virtual work which the work is done by imaginary or virtual displacements.

$$\delta W = \iiint_V \sigma_{ij} \delta \varepsilon_{ij} dV + \iiint_A F_j \delta u_j dV + \iint_A T \delta u_j dA \tag{16}$$

where, ε is the strain, σ is the stress, F is the body force, δu is the virtual displacement, and T is the traction on surface A. The symbol δ is the variational operator designating the virtual quantity . Finite element interpolation for displacement field [15]

$$\{u\} = [N]\{\hat{u}\} \tag{17}$$

where is $\{u\}$ u displacement vector of arbitrary point and $\{\hat{u}\}$ is nodal displacement point's vector. $[N]$ is shape function matrix. After FEM procedure the problem is reduced to the solution of the linear system of equations

$$[K_e]\cdot\{u\}=\{f\} \tag{18}$$

where are $\{u\}$ is global displacement vector, $\{f\}$ - global nodal force vector, and $[K_e]$ - global stiffness matrix. Finite element analyses were performed for computer generated network of 100 fibers. The comparison of calculated data with experimental data [10] for nanotube sheet shows some discrepancies (Figure 14). A rough morphological network model for the sheets can explain this on the one hand and simple joint morphology on the other hand [16].

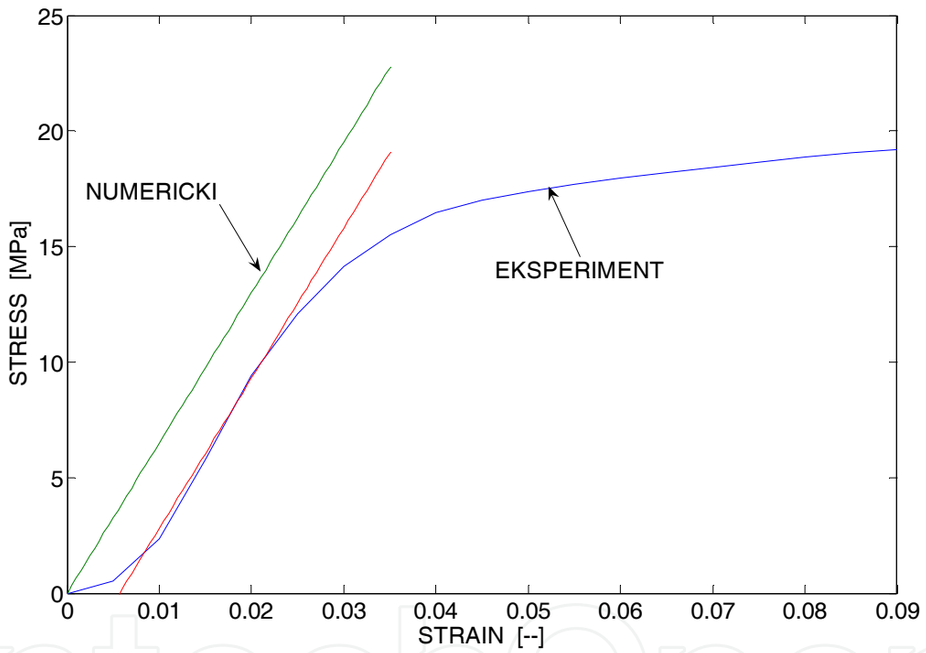

Fig. 14. The stress-strain curve [10]

4.3 Flow in fibre network

Electrospun nanofiber materials are becoming an integral part of many recent applications and products. Such materials are currently being used in tissue engineering, air and liquid filtration, protective clothing's, drug delivery, and many others. Permeability of fibrous media is important in many applications, therefore during the past few decades, there have been many original studies dedicated to this subject. Depending on the fiber diameter and the air thermal conditions, there are four different regimes of flow around a fiber:

a) Continuum regime ($K_N \le 10^{-3}$),

b) Slip-flow regime ($10^{-3} \le K_N \le 0.25$),

c) Transient regime ($0.25 \le K_N \le 10$).

d) Free molecule regime ($K_N \ge 10$),

Here, $K_N = 2\lambda / d$ is the fiber Knudson number, where $\lambda = RT / \sqrt{2}\hat{N}\pi \cdot d^2 p$ is the mean free path of gas molecules, d is fiber diameter, $\hat{N}$ is Avogadro number. Air flow around most electrospun nanofibers is typically in the slip or transition flow regimes. In the context of air filtration, the 2D analytical work of Kuwabara [17] has long been used for predicting the permeability across fibrous filters. The analytical expression has been modified by Brown [18] to develop an expression for predicting the permeability across filter media operating in the slip flow regime. The ratio of the slip to no-slip pressure drops obtained from the simplified 2D models may be used to modify the more realistic, and so more accurate, existing 3D permeability models in such a way that they could be used to predict the permeability of nanofiber structure. To test this supposition, for above developed 3D virtual nanofibrous structure, the Stokes flow equations solved numerically inside these virtual structures with an appropriate slip boundary condition that is developed for accounting the gas slip at fiber surface. Our results leading to the development of a correction factor for the available analytical permeability models of 3D fibrous media are presented.

4.3.1 Flow field calculation

A steady state, laminar, incompressible model has been adopted for the flow regime inside our virtual media. Implemented in the Fluent code [19] is used to solve continuity and conservation of linear momentum in the absence of inertial effects

$$\nabla \cdot v = 0 \tag{19}$$

$$\nabla p = \mu \cdot \Delta^2 v \tag{20}$$

The grid size required to mesh the gap between two fibers around their crossover point is often too small. The computational grid used for computational fluid dynamics (CFD) simulations needs to be fine enough to resolve the flow field in the narrow gaps, and at the same time coarse enough to cover the whole domain without requiring infinite computational power. Permeability of a fibrous material is often presented as a function of fiber radius, *r*, and solid volume fraction α , of the medium. Here, we use the continuum regime analytical expressions of Jackson and James [20], developed for 3D isotropic fibrous structures given as

$$k / r^2 = \frac{3r^2}{20\alpha}\left[-\ell n(\alpha) - 0.931\right] \tag{21}$$

Brown [18] has proposed an expression for the pressure drop across a fibrous medium based on the 2D cell model of Kuwabara [17] with the slip boundary condition

$$\Delta p_{SLIP} = \frac{4\mu\alpha \cdot hV \cdot \left(1 + 1.996K_N\right)}{r^2\left[\hat{K} + 1.996K_N\left(. - 0.5 \cdot \ell n\alpha - 0.25 + 0.25\alpha^2\right)\right]} \tag{22}$$

where $\hat{K} = -0.5 \cdot \ell n\alpha - 0.75 + \alpha - 0.25\alpha^2$ Kuwabara hydrodynamic factor, h is fabric thickness, and V is velocity. As discussed in the some reference [*], permeability (or pressure drop) models obtained using ordered 2D fiber arrangements are known for under-predicting the permeability of a fibrous medium. In order to overcome this problem, if a correction factor can be derived based on the above 2D expression, and used with the realistic expressions developed for realistic 3D fibrous structures. From equation (22) we have for the case of no-slip boundary condition ($K_N = 0$):

$$\Delta p_{NONSLIP} = \frac{4\mu\alpha \cdot hV}{r^2\hat{K}} \tag{23}$$

Here, we define our correction factor as

$$\Xi = \frac{\Delta p_{NONSLIP}}{\Delta p_{SLIP}} \tag{24}$$

to be used in modifying the original permeability expressions of Jackson and James[19],Jackson and James, 1986 G. Jackson and D. James, The permeability of fibrous porous media, *The Canadian Journal of Chemical Engineering* **64** (1986), p. 364. **Full Text** via CrossRef | View Record in Scopus | Cited By in Scopus (204) and/or any other expression based on the no-slip boundary condition, in order to incorporate the slip effect. For instance, the modified expression of Jackson and James can be presented as

$$k_z = \frac{3r^2}{20\alpha}\left[-\ell n(\alpha) - 0.931\right] \cdot \Xi \tag{25}$$

operating pressure has no influence on the pressure drop in the continuum region, while pressure drop in the free molecular region is linearly proportional to the operating pressure. While there are many equations available for predicting the permeability of fibrous materials made up of coarse fibers, there are no accurate “easy-to-use” permeability expressions that can be used for nanofiber media. On Fig. 15 are drown corrected Jackson and James data (blue line). Points on figure are CFD numerical data.

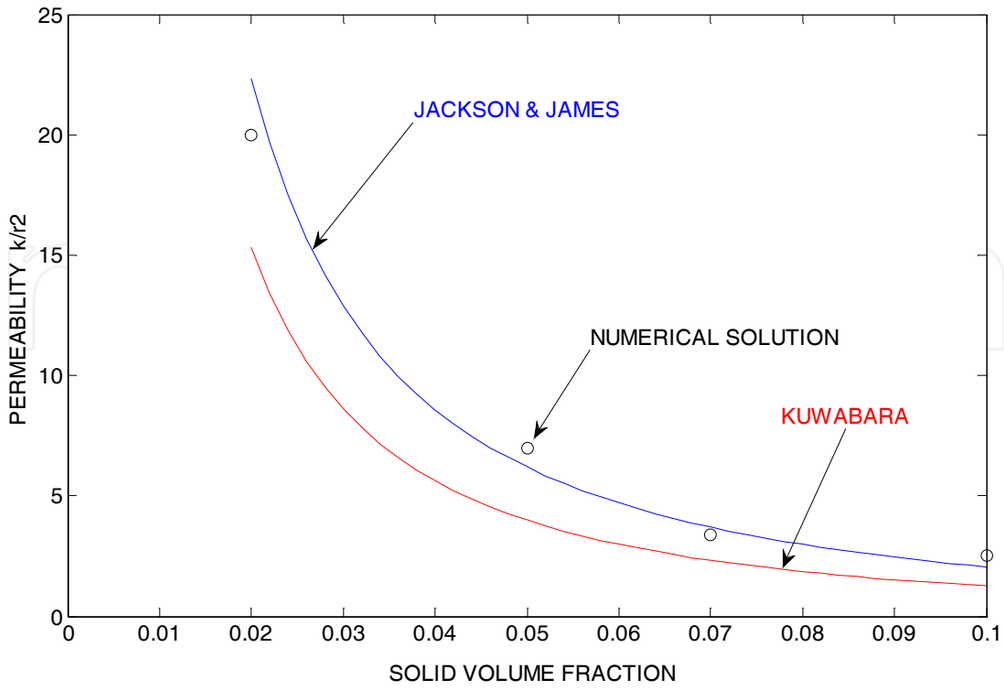

Fig. 15. Permeability k / r^2 dependence on solid volume fraction α

4.4 Some illustrative examples

4.4.1 FUEL CELL EXAMPLE

A Yttria stabilized zirconia were formed in an electrospinning process. The electrospun fibers were calcinated at temperature more then 1000°C and finally coated with nickel in electroless plating process. This novel material can be applied as anode for the solid oxide fuel cells.

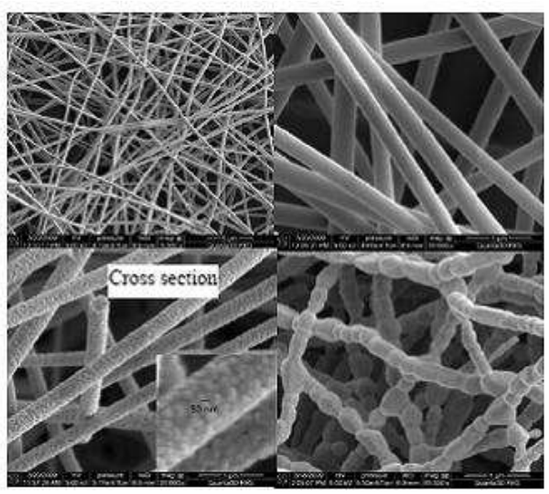

Fig. 16. FEG –SEM image

4.4.2 PROTECTIVE CLOTHING EXAMPLE

The development of smart nanotextiles has the potential to revolutionize the functionality of our clothing and the fabrics in our surroundings. This is made possible by such developments as new materials, fibbers, and finishing; inherently conducting polymers; carbon nanotubes; and antimicrobial nanocoatings. These additional functionalities have numerous applications in healthcare, sports, military applications, fashion, at.. Smart textiles become a critical part of the emerging area of body sensor networks incorporating sensing, actuation, control and wireless data transmission.

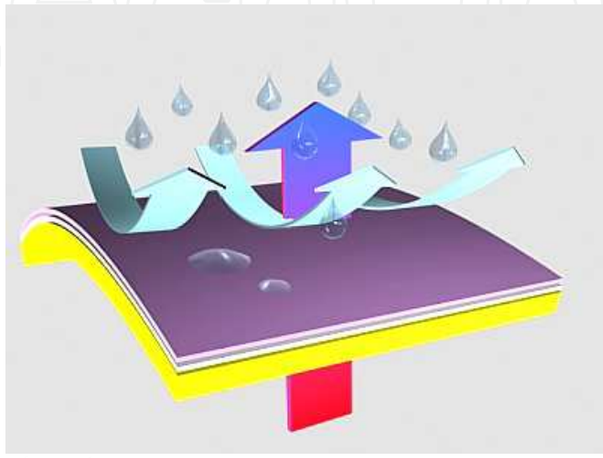

Fig. 17. Ultrathin layer for selective transport

4.4.3 MEDICAL DEVICE

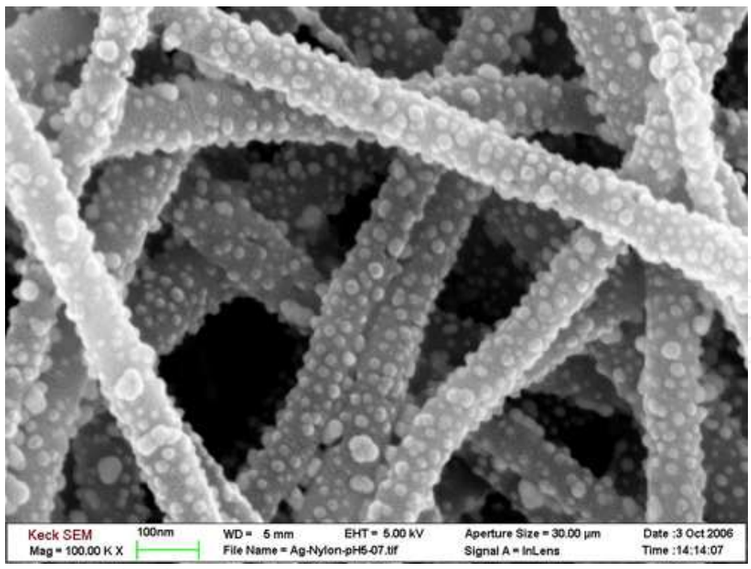

Fig. 18. Cotton coated with silver

Basic engineered nanomaterial and biotechnology products will be enormously useful in future medical applications. We know nanomedicine as the monitoring, repair, construction and control of biological systems at the nanoscale level, using engineered nanodevices and

nanostructures. The upper portion of the dress contains cotton coated with silver nanoparticles. Silver possesses natural antibacterial qualities that are strengthened at the nanoscale, thus giving the ability to deactivate many harmful bacteria and viruses. The silver infusion also reduces the need to wash the garment, since it destroys bacteria, and the small size of the particles prevents soiling and stains.

5. Conclusion

Electrospinning is a simple, versatile, and cost-effective technology which generates non-woven fibers with high surface area to volume ratio, porosity and tunable porosity. Because of these properties this process seems to be a promising candidate for various applications especially nanostructure applications. Electrospun fibers are increasingly being used in a variety of applications such as, tissue engineering scaffolds, wound healing, drug delivery, immobilization of enzymes, as membrane in biosensors, protective clothing, cosmetics, affinity membranes, filtration applications etc. In summary, mother Nature has always used hierarchical structures such as capillaries and dendrites to increase multifunctional of living organs. Material scientists are at beginning to use this concept and create multiscale structures where nanotubes, nanofillers can be attached to larger surfaces and subsequently functionalized. In principle, many more applications can be envisioned and created. Despite of several advantages and success of electrospinning there are some critical limitations in this process such as small pore size inside the fibers. Several attempts in these directions are being made to improve the design through multilayering, inclusion of nanoelements and blending with polymers with different degradation behaviour. As new architectures develop, a new wave of surface-sensitive devices related to sensing, catalysis, photo-voltaic, cell scaffolding, and gas storage applications is bound to follow.

6. References

[1] Sanchez, C. , Arribart, H., Guille, G.M.M, biomimetism and bioinspiration as tools for the design of innovative materials and systems, Nature Materials, 4 (2005) 277-238.

[2] Ko, F. K., Gogotsi, Y., Ali, A., Naguib, N., Ye, H., Yang, G., Li, C. and Willis, P. Electrospinning of continuous Carbon Nanotube-Filled Nanofiber Yarns, Adv. Materials, 2003, 15, 1161.

[3] Zhao, Y. Jiang, L. Hollow micro/nanomaterials with multilevel interior structures, Advanced Materials, 21 (2009) 1-18.

[4] Hohman, M. M., Shin, M., Rutledge, G., Brenner, M.P., Electrospinning and electrically forced jets, I & II, Physics of Fluids, 2001, 13, 2201.

[5] Huang, Z. M., Zhang, Y. Z., Kotaki, M. and Ramakrishna, S., A review on polymer nanofibers by electrospinning and their applications in nanocomposites, Composites Sciences. and Technology, 2003, 63, 2223.

[6] Song, Y. S. and Youn, J. R., Modeling of rheological behavior of nanocomposites by Brownnian dynamics simulation, Korea-Australia Rheology J., 2004, 16, 201.

[7] Dror, Y., Salalha, W., Khalfin, R. L. Cohen, Y. Yarin, A. L. and Zussman, E.,. Carbon nanotubes embedded in oriented polymer nanofibers by electrospinning, Langmuir, 2003, 19, 7012.

[8] Folgar, F.Tucker, C. L. Orientation Behavior of Fibers in Concentrated Suspensions, J. of Reinforced Plastics and Composites, (1984),3, 98-119.
[9] Gates, T. S., Odegard, G. M., Frankland, S. J. V. and Clancy, T. C., Computational materials: Multi-scale modeling and simulation of nanostructured materials, Composite Science and Technology, 2005, 65, 2416.
[10] Agic, A. Multiscale mechanical phenomena in electrospun carbon nanotube composites, J. of Appl. Polymer Science, 108 (2008) 1191-1200.
[11] Gao, X. L., Li, K., A shear-lag model for carbon nanotube-reinforced polymer composites, Int. J. of Solids and Struct., 2005, 42, 1649.
[12] Agić, A., Mijović, B. Polymer structure on multiple material scales, Polymeric materials and Aditives (ed. Ivankovic, M.) Croatian Society for Rubber and Plastic, Zagreb, (2009) 75-87.
[13] Teo, W.E, Ramakrishna, S**.** Electrospun nanofibers as a platform for multifunctional, hierarchically organized nanocomposite, Composites Science and Technology, 69 (2009) 1804-1816.
[14] Silling, S. A. and Bobaru, F., Peridynamics modeling of membranes and fibers, Int. J. Non-linear Mechanics, 2005, 40, 395.
[15] Berhan, L., Yi, Y. B., Sastry, A. M., Munoz, E., Selvidge, M. and Baughman, R., Mechanical properties of nanotube sheets: Alterations in joint morphology and achievable moduli in manufacturable materials, J. of Appl. Physics, 2004, 95, 4335.
[16] Heyden, S., 2003. *Network modelling for the evaluation of mechanical properties of cellulose fibre fluff,* Ph.D., Lund University.
[17] S. Kuwabara, The forces experienced by randomly distributed parallel circular cylinders of spheres in a viscous flow at small Reynolds number, Journal of the Physical Society of Japan **14** (1959), 527–532.
[18] R.C. Brown, *Air Filtration, Pergamon Press, Oxford (1993).*
[19] FLUENT 6.2 User's Guide, www.fluent.com
[20] Jackson, G. James, D. The permeability of fibrous porous media. The Canadian Journal of Chemical Engineering, 64 (1986) 364-373.

Engineering the Future
Edited by Laszlo Dudas

ISBN 978-953-307-210-4
Hard cover, 414 pages
Publisher Sciyo
Published online 02, November, 2010
Published in print edition November, 2010

This book pilots the reader into the future. The first three chapters introduce new materials and material processing methods. Then five chapters present innovative new design directions and solutions. The main section of the book contains ten chapters organized around problems and methods of manufacturing and technology, from cutting process optimisation through maintenance and control to the Digital Factory. The last two chapters deal with information and energy, as the foundations of a prospering economy.

How to reference
In order to correctly reference this scholarly work, feel free to copy and paste the following:

Ante Agic and Budimir Mijovic (2010). Multifunctional Product Design by Nanostructures, Engineering the Future, Laszlo Dudas (Ed.), ISBN: 978-953-307-210-4, InTech, Available from: http://www.intechopen.com/books/engineering-the-future/multifunctional-product-design-by-nanostructures

INTECH
open science | open minds

InTech Europe
University Campus STeP Ri
Slavka Krautzeka 83/A
51000 Rijeka, Croatia
Phone: +385 (51) 770 447
Fax: +385 (51) 686 166
www.intechopen.com

InTech China
Unit 405, Office Block, Hotel Equatorial Shanghai
No.65, Yan An Road (West), Shanghai, 200040, China
中国上海市延安西路65号上海国际贵都大饭店办公楼405单元
Phone: +86-21-62489820
Fax: +86-21-62489821

IntechOpen